JOC*Article*

Conformational Rigidification via Derivatization Facilitates the Determination of Absolute Configuration Using Chiroptical Spectroscopy: A Case Study of the Chiral Alcohol *endo*-Borneol

F. J. Devlin and P. J. Stephens*

Department of Chemistry, University of Southern California, Los Angeles, California 90089-0482

P. Besse

Laboratoire SEESIB, UMR 6504 du CNRS, Université Blaise Pascal, 63177 Aubière Cedex, France

pstephen@usc.edu

Received December 2, 2004

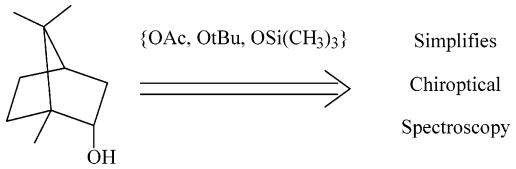

We demonstrate that derivatization of the OH group of *endo*-borneol, **1**, leads to conformational rigidification. Conformational analysis (CA) of **1** and its methyl, acetate, *tert*-butyl, and trimethylsilyl derivatives, **2**−**5**, is carried out using ab initio density functional theory (DFT). The number of thermally accessible stable conformations is reduced from 3 in **1**, to 2 in **2**, and to 1 in **3**−**5**. Comparison of IR and vibrational circular dichroism (VCD) spectra of **1** and **3**−**5**, calculated using DFT, to experimental spectra unambiguously confirms the DFT CA. The determination of absolute configurations (ACs) of chiral molecules via analysis of chiroptical spectra using DFT methods increases in complexity and decreases in reliability as the number of populated conformations increases. Our results for *endo*-borneol support the conclusion that, in the case of chiral alcohols, derivatization can lead to substantial rigidification and, as a result, significantly facilitate the determination of ACs.

Introduction

In recent years, it has become practicable to calculate the chiroptical properties of chiral molecules using ab initio density functional theory (DFT).[1] As a result, the absolute configurations (ACs) of chiral molecules are increasingly being determined using chiroptical methods in combination with DFT calculations.[2] This development occurred first in the case of the vibrational circular dichroism (VCD) phenomenon.[1a,b,2a−h] Subsequently, it has taken place for the optical rotation (OR)[1c−h,2i−m] and electronic circular dichroism (ECD)[1i,j,2k,l] phenomena. The methodology for determining ACs is fundamentally simple. A chiroptical property of the target molecule is predicted for the two possible enantiomers. Comparison of the predictions to the experimental data for a sample of known specific rotation then defines for which enantiomer calculation and experiment are in agreement and, hence, the AC of the sample.

For a conformationally rigid molecule, exhibiting only one thermally accessible stable conformation, this procedure is straightforward and limited in reliability only by the reliability of the DFT methodology in calculating chiroptical properties. For conformationally flexible molecules, exhibiting multiple thermally accessible conformations, the prediction of the observable chiroptical property involves averaging over the contributions of the populated conformations. Thus, the property $P(\nu)$ at

(1) (a) Cheeseman, J. R.; Frisch, M. J.; Devlin, F. J.; Stephens, P. J. *Chem. Phys. Lett*. **1996**, *252*, 211−220. (b) Stephens, P. J.; Ashvar, C. S.; Devlin, F. J.; Cheeseman, J. R.; Frisch, M. J. *Mol. Phys.* **1996**, *89*, 579−594. (c) Stephens, P. J.; Devlin, F. J.; Cheeseman, J. R.; Frisch M. J. *J. Phys. Chem. A* **2001**, *105*, 5356−5371. (d) Mennucci, B.; Tomasi, J.; Cammi, R.; Cheeseman, J. R.; Frisch, M. J.; Devlin, F. J.; Gabriel, S.; Stephens, P. J. *J. Phys. Chem. A* **2002**, *106*, 6102−6113. (e) Grimme, S. *Chem. Phys. Lett*. **2001**, *339*, 380−388. (f) Grimme, S.; Furche, F.; Ahlrichs, R. *Chem. Phys. Lett*. **2002**, *361*, 321−328. (g) Autschbach, J.; Patchkovskii, S.; Ziegler, T.; van Gisbergen, S. J. A.; Baerends, E. J. *J. Chem. Phys*. **2002**, *117*, 581−592. (h) Ruud, K.; Helgaker, T. *Chem. Phys. Lett*. **2002**, *352*, 533−539. (i) Furche, F.; Ahlrichs, R.; Wachsmann, C.; Weber, E.; Sobanski, A.; Vogtle F.; Grimme, S. *J. Am. Chem. Soc*. **2000**, *122*, 1717−1724. (j) Autschbach, J.; Ziegler, T.; van Gisbergen, S. J. A.; Baerends, E. J. *J. Chem. Phys.* **2002**, *116*, 6930−6940.

10.1021/jo0478611 CCC: $30.25
Published on Web 03/17/2005

optical frequency ν of a flexible molecule can be written

$$P(\nu) = \sum_i x_i [P(\nu)]_i$$

where $[P(\nu)]_i$ is the value of $P(\nu)$ for the ith conformation, whose fractional equilibrium population is $x_i (\sum_i x_i = 1)$.

Conformational populations, x_i, can be calculated (e.g., using DFT) or measured (e.g., using NMR), but in either case (and especially in the former case) uncertainties will exist. As a result, predicted conformationally averaged chiroptical properties suffer from additional uncertainties. These added uncertainties may lead to unreliability of an AC derived from chiroptical data. For example, if a molecule exhibits two conformations of similar energy and if the two conformations exhibit specific rotations, $[\alpha]_\nu$, of similar magnitude but of opposite sign, the sign of the conformationally averaged $[\alpha]_\nu$ value depends sensitively on the conformational populations and small errors in the populations can lead to an erroneous sign. It follows that whichever AC is deduced, it is unreliable. Thus, broadly, the application of chiroptical methods in conjunction with DFT calculations becomes increasingly unreliable as the number of populated conformations increases.

In this paper, we discuss a strategy for diminishing the problem of conformational flexibility via chemical derivatization. The basic idea, which is very simple, is to add a bulky group to the molecule of interest, without affecting its absolute stereochemistry, in such a way as to diminish the number of accessible conformations. By way of example, we focus specifically on alcohols. In general, the OH group of an alcohol can rotate relatively freely around the adjacent C−O bond and there will be multiple stable conformations. If the H atom of the OH group is replaced by a bulky group X, steric hindrance to rotation of the OX group is likely to be much greater, limiting the number of stable conformations which are accessible. In this work, the degree to which such derivatization leads to conformational rigidification has been explored for the specific chiral alcohol *endo*-borneol, **1**:

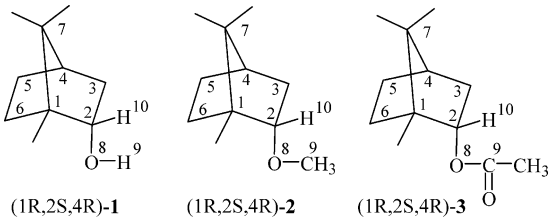

(1R,2S,4R)-**1** (1R,2S,4R)-**2** (1R,2S,4R)-**3**

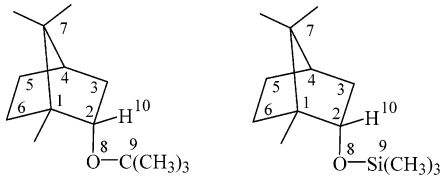

(1R,2S,4R)-**4** (1R,2S,4R)-**5**

The derivatives of borneol which have been studied are the methyl, acetate, *tert*-butyl, and trimethylsilyl derivatives, **2**−**5**. We have first predicted the number and relative energies of the stable conformations of **1**−**5** using DFT. Then, we have measured the IR and VCD spectra of **1**, **3**, **4**, and **5** in the mid-IR spectral region and predicted the IR and VCD spectra of **1**, **3**, **4**, and **5** using DFT. Lastly, we have compared the calculated and experimental IR and VCD spectra of **1**, **3**, **4**, and **5** to assess the reliability of the DFT conformational analyses for these molecules. Our results demonstrate that conformational rigidification indeed occurs on derivatization of the OH group of *endo*-borneol and permit evaluation of the relative utilities of the methyl, acetate, *tert*-butyl, and trimethylsilyl derivatives in achieving maximum rigidification.

In the case of alcohols, derivatization provides an added benefit, in addition to conformational rigidification. As is well-known, intermolecular hydrogen (H) bonding between alcohol molecules is strong and solutions of alcohols exhibit aggregation with increasing concentration. Chiroptical spectra are then concentration-dependent, and spectra measured at medium-to-high concentrations contain contributions not only from monomeric alcohol molecules but also from dimers and higher aggregates. An example of concentration dependence in the chiroptical spectra of alcohols is provided by the VCD of the methine C−H stretching vibration in Ph·CH(OH)·CF_3, whose signs in the neat liquid and dilute CCl_4 solution spectra are opposite.[3] In principle, meaningful comparison of spectra calculated for monomeric alcohol molecules alone to experimental spectra is then not possible. Derivatization eliminating intermolecular H-bonding removes this problem and permits meaningful comparison of calculated spectra to experimental spectra measured at much higher concentrations than possible for the parent alcohol. Here, we document this fringe benefit of derivatization via studies of the concentration dependence of the IR spectra of **1**, **3**, **4**, and **5**.

Methods

IR and VCD Spectroscopy. IR spectra of CCl_4 solutions of the (+)- and (−)-enantiomers of **1**, **3**, and **5** were obtained at a resolution of 1 cm^{-1}. VCD spectra were obtained using Bomem/BioTools Chiral IR spectrometers at a resolution of 4 cm^{-1}. VCD scans were 1 h. For **4** (obtained using the method of Armstrong et al.[4]) the VCD spectrometer was fitted with a Dual PEM accessory.[5] KBr cells of path lengths 109, 239, and

(2) (a) Stephens, P. J.; Devlin, F. J. *Chirality* **2000**, *12*, 172−179. (b) Aamouche, A.; Devlin, F. J.; Stephens, P. J. *J. Am. Chem. Soc.* **2000**, *122*, 2346−2354. (c) Aamouche, A.; Devlin, F. J.; Stephens, P. J. *J. Am. Chem. Soc.* **2000**, *122*, 7358−7367. (d) Aamouche, A.; Devlin, F. J.; Stephens, P. J.; Drabowicz, J.; Bujnicki, B.; Mikolajczyk, M. *Chem.−Eur. J.* **2000**, *6*, 4479−4486. (e) Stephens, P. J.; Aamouche, A.; Devlin, F. J.; Superchi, S.; Donnoli, M. I.; Rosini, C. *J. Org. Chem.* **2001**, *66*, 3671−3677. (f) Devlin, F. J.; Stephens, P. J.; Scafato, P.; Superchi, S.; Rosini, C. *Chirality* **2002**, *14*, 400−406. (g) Devlin, F. J.; Stephens, P. J.; Oesterle, C.; Wiberg, K. B.; Cheeseman, J. R.; Frisch, M. J. *J. Org. Chem.* **2002**, *67*, 8090−8096. (h) Ceré, V.; Peri, F.; Pollicino, S.; Ricci, A.; Devlin, F. J.; Stephens, P. J.; Gasparrini, F.; Rompietti, R.; Villani, C. *J. Org. Chem.* **2005**, *70*, 664−669. (i) Stephens, P. J.; Devlin, F. J.; Cheeseman, J. R.; Frisch, M. J.; Rosini, C. *Org. Lett.* **2002**, *4*, 4595−4598. (j) Stephens, P. J.; Devlin, F. J.; Cheeseman, J. R.; Frisch, M. J.; Bortolini, O.; Besse, P. *Chirality* **2003**, *15*, S57−S64. (k) Stephens, P. J.; McCann, D. M.; Butkus, E.; Stoncius, S.; Cheeseman, J. R.; Frisch, M. J. *J. Org. Chem.* **2004**, *69*, 1948−1958. (l) Stephens, P. J.; McCann, D. M.; Devlin, F. J.; Cheeseman, J. R.; Frisch, M. J. *J. Am. Chem. Soc.* **2004**, *126*, 7514−7521. (m) McCann, D. M.; Stephens, P. J.; Cheeseman, J. R. *J. Org. Chem.* **2004**, *69*, 8709−8717.

(3) Nafie, L. A.; Keiderling, T. A.; Stephens, P. J. *J. Am. Chem. Soc.* **1976**, *98*, 2715−2723.

(4) Armstrong, A.; Brackenridge, I.; Jackson, R. F. W.; Kirk, J. M. *Tetrahedron Lett.* **1988**, 2483−2486.

(5) Nafie, L. A. *Appl. Spectrosc.* **2000**, *54*, 1634−1645.

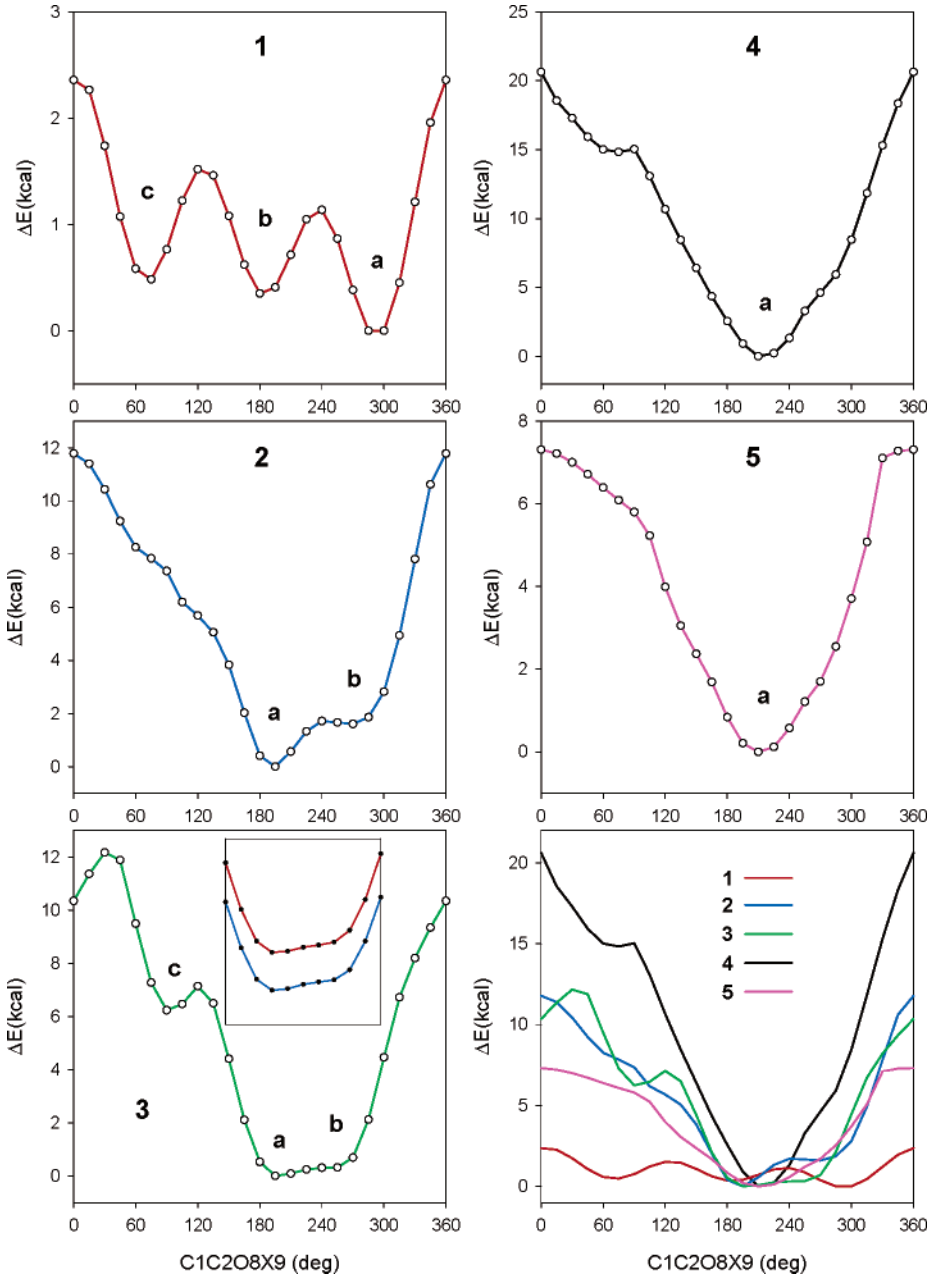

FIGURE 1. B3LYP/6-31G* Potential energy surface scans for (1*R*,2*S*,4*R*)-*endo*-borneol-OX. OX = OH (**1**), OCH_3 (**2**), $OCOCH_3$ (**3**), $OC(CH_3)_3$ (**4**), and $OSi(CH_3)_3$ (**5**). For **3**, limited B3LYP/TZ2P (blue) and B3PW91/TZ2P (red) scans are also shown.

597 μ were used. Baselines for IR spectra were solvent spectra. In the absence of racemic samples of **1**, **3**, **4**, and **5** and given different ee values for (+) and (−) samples, VCD spectra were collected and processed as follows. VCD spectra were measured for (+) and (−) samples of closely similar concentrations, c_+ and c_-. Assuming that absorbance artifacts in (+) and (−) VCD spectra are identical, it is easy to show that

$$\Delta A_+ - \Delta A_- = \Delta\epsilon_+^{OP} ee_+ [c_+ + c_-(ee_-/ee_+)]l \qquad (1)$$

where ΔA_+ and ΔA_- are the measured VCD of the (+) and (−) samples, whose ee values are ee_+ and ee_-, respectively, $\Delta\epsilon_+^{OP}$ is the $\Delta\epsilon$ of the optical pure (+)-enantiomer, and l is the cell path length. The ratio of ee values, ee_-/ee_+, was taken to be the ratio of the $[\alpha]_D$ values of the (−) and (+) samples, measured on the solutions used to measure the VCD spectra. Thus, from $\Delta A_+ - \Delta A_-$, c_+, c_-, $[\alpha]_D(-)/[\alpha]_D(+)$, and l, we can obtain $\Delta\epsilon_+^{OP} ee_+$, the VCD spectrum of the (+) enantiomer. As discussed above, ee values for the (+)-enantiomers of **1**, **3**, **4**, and **5** are in all cases >99% and $\Delta\epsilon_+^{OP} ee_+$ is very close to $\Delta\epsilon_+^{OP}$. In Figure 3, experimental VCD spectra of the (+) enantiomers of **1**, **3**, **4**, and **5** are reported as $\Delta\epsilon_+^{OP} ee_+$.

Ab Initio DFT Calculations. Potential energy surface (PES) scans of **1**−**5** were carried out using DFT at the B3LYP/6-31G* level using GAUSSIAN 98 or 03.[6] Equilibrium geometries and energies of stable conformations identified from the PES scans were then obtained at the B3LYP/6-31G*, B3LYP/TZ2P, and B3PW91/TZ2P levels. Harmonic vibrational frequencies were calculated at all three levels and, thence, free energies of all stable conformations. Atomic polar tensors (APTs) and atomic axial tensors (AATs) were also calculated at the B3LYP/TZ2P and B3PW91/TZ2P levels leading to harmonic vibrational dipole strengths and rotational strengths.[2a,b] IR and VCD spectra were simulated using calculated harmonic frequencies, dipole strengths, and rotational strengths, together with Lorentzian band shapes (γ = 4.0 cm^{-1}).[7]

TABLE 1. Geometries, Relative Energies and Free Energies, and Populations of the conformations of 1, 3, 4, and 5

	dihedral angles (C1C2O8X9)[a]			ΔE[b]			ΔG[b]			P (%)[c]		
	B3LYP		B3PW91	B3LYP		B3PW91	B3LYP		B3PW91	B3LYP		B3PW91
	6-31G*	TZ2P	TZ2P	6-31G*	TZ2P	TZ2P	6-31G*	TZ2P	TZ2P	6-31G*	TZ2P	TZ2P
1a: X = H	293	288	288	0.00	0.00	0.00	0.00	0.00	0.00	50.3	44.3	43.1
1b: X = H	185	190	189	0.39	0.26	0.32	0.31	0.14	0.18	29.5	34.9	31.6
1c: X = H	71	70	69	0.53	0.55	0.47	0.53	0.44	0.31	20.2	20.8	25.3
3a: X = C	197	198	198	0.00			0.00			54.3	100.0	100.0
3b: X = C	255			0.34			0.10			45.7		
4a: X = C	214	216	215								100.0	100.0
5a: X = Si	213	220	219								100.0	100.0

[a] Angles are in degrees. AC is 1*R*,2*S*,4*R*. [b] ΔE and ΔG are in kcal/mol. [c] Populations are based on ΔG values; T = 293 K.

Sodium D line specific rotations, $[\alpha]_D$, were calculated at the equilibrium geometries of stable conformations of **1**−**5** using the time-dependent DFT with GIAOs (TDDFT/GIAO) methodology[1c,d] via GAUSSIAN 03 at the B3LYP/aug-cc-pVDZ and B3PW91/aug-cc-pVDZ levels.

All calculations were carried out for the 1*R*,2*S*,4*R* ACs of **1**−**5**.

Results

Conformational Analysis. Conformational analysis of **1** and its derivatives **2**−**5** has been carried out at the B3LYP/6-31G* level. Energy scans with respect to the dihedral angle C1C2O8X9, where X = H, C, C, C, and Si in **1**, **2**, **3**, **4**, and **5**, respectively, are shown in Figure 1. In the case of **3**, the planar acetate group C2O8C9═O is in the more stable cis conformation.[2g] For **1**, three well-defined minima, **1a**−**c**, are observed as C1C2O8H9 is varied over 360°, as anticipated. The barriers between minima are small: the maximum variation in energy is 2.4 kcal/mol. For **2**−**5**, the variation in energy is much larger. In the case of **2**, the maximum variation is 11.8 kcal/mol. Two minima, **a** and **b**, are observed. In the case of **3**, the maximum variation in energy is 12.2 kcal/mol. Three minima are observed: two, **a** and **b**, are similar in energy and separated by a very small barrier; the third, **c**, is much higher in energy (>5 kcal/mol). In the case of **4**, the maximum variation in energy is 20.6 kcal/mol. Only one minimum, **a**, is observed (we disregard the shallow minimum apparent at ∼15 kcal/mol). In the case of **5**, the maximum variation in energy is 7.3 kcal/mol. Again, only one minimum, **a**, is observed.

For **1**, **3**, **4**, and **5**, we have further calculated the structures and energies of the stable conformations shown to exist by the energy scans. Geometry optimization was first carried out at the B3LYP/6-31G* level. Subsequently, geometries obtained were further optimized at the B3LYP/TZ2P and B3PW91/TZ2P levels. Harmonic vibrational frequency calculations confirmed that all structures were stable conformations and, in addition, permitted the calculation of conformational free energies. The key dihedral angles, C1C2O8X9, for all conformations, together with their relative energies and free energies, are tabulated in Table 1. The B3PW91/TZ2P structures are shown in Figure 2. In the case of **1**, there are three stable conformations, in each of which the O−H bond is staggered with respect to the C2−C1, C2−C3, and C2−H10 bonds. For the most stable conformation, **1a**, the O−H bond lies between the C2−C1 and C2−H10 bonds. In conformations **1b** and **1c**, the O−H bond lies between the C2−C3 and C2−H10 bonds and between the C2−C1 and C2−C3 bonds, respectively. The three conformations vary little in energy; relative energies and relative free energies are very similar. The B3LYP and B3PW91 functionals give very similar structures and relative energies.

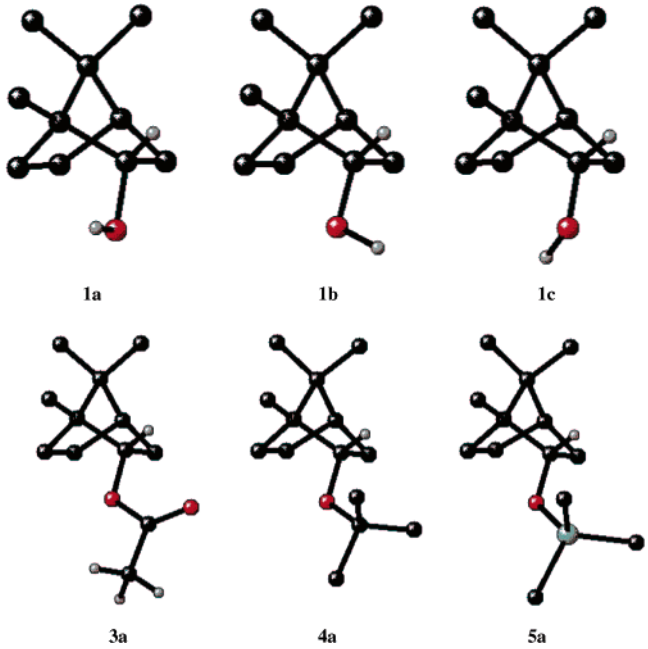

FIGURE 2. B3PW91/TZ2P geometries for the 1*R*,2*S*,4*R* ACs of **1a**, **1b**, **1c**, **3a**, **4a**, and **5a**.

In the case of **3**, geometry optimization at the B3LYP/6-31G* level leads to two low-energy, stable conformations, **a** and **b**, differing in energy by 0.34 kcal/mol. However, reoptimization of these two structures at the TZ2P basis set level, for both B3LYP and B3PW91 functionals, leads to a single structure, **a**, similar to the B3LYP/6-31G* conformation of lower energy. This shows that at the higher basis set level, there exists only one stable low-energy conformation. To confirm this conclusion, we have rescanned the lower energy portion of the potential energy surface of **3** at both B3LYP/TZ2P and B3PW91/TZ2P levels, with the results shown in Figure 1. As anticipated, evidence for a second conformation is

(6) *Gaussian 98/03*, Gaussian Inc., Wallingford, CT, www.gaussian.com.

(7) (a) Devlin, F. J.; Stephens, P. J.; Cheeseman, J. R.; Frisch, M. J. *J. Phys. Chem.* **1997**, *101*, 6322−6333. (b) Devlin, F. J.; Stephens, P. J.; Cheeseman, J. R.; Frisch, M. J. *J. Phys. Chem.* **1997**, *101*, 9912−9924.

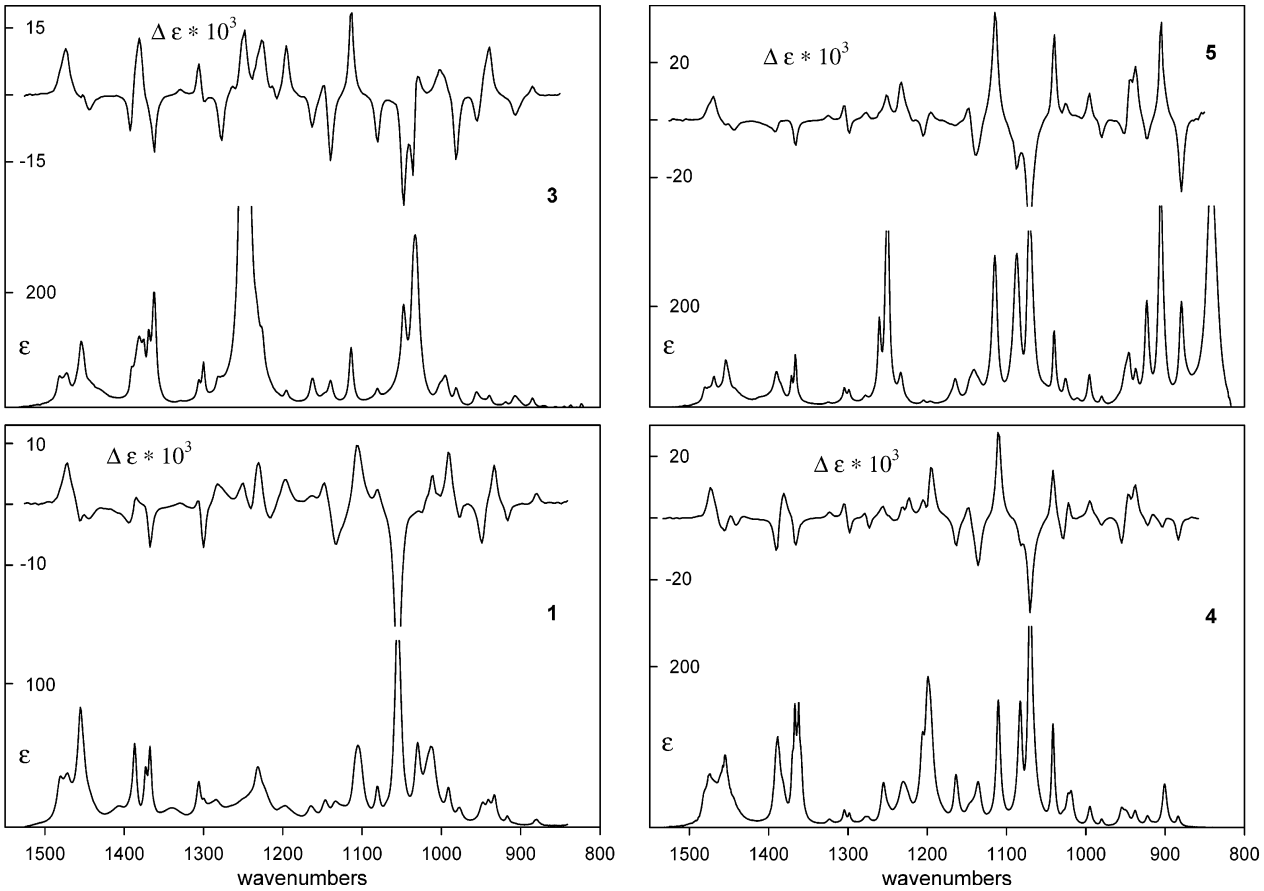

FIGURE 3. Experimental IR and VCD spectra of CCl_4 solutions of **1**, **3**, **4**, and **5** in the mid-IR spectral region. The VCD spectra are for the (+)-enantiomers (see Methods). **1**: IR (+)-**1**, 0.19 M, path length 597 μ; VCD (+)-**1**, 0.19 M, path length 597 μ (1526−840 cm^{-1}). **3**: IR (+)-**3**, 0.20 M, path length 109 μ; VCD (+)-**3**, 0.20 M, path length 597 μ (1526−850 cm^{-1}) except 109 μ (1269−1203 cm^{-1}) and 239 μ (1054−1010 cm^{-1}). **4**: IR (+)-**4**, 0.15 M, path length 597 μ; VCD (+)-**4**, 0.15 M, path length 597 μ (1533−858 cm^{-1}) except 239 μ (1232−1188 cm^{-1}, 1117−1038 cm^{-1}). **5**: IR (+)-**5**, 0.15 M, path length 239 μ; VCD (+)-**5**, 0.15 M, path length 597 μ (1526−850 cm^{-1}) except 109 μ (1261−1217 cm^{-1}) and 239 μ (1144−1032 cm^{-1}, 948−850 cm^{-1}).

less pronounced at the higher basis set level. The B3LYP/6-31G* scan for **3** also indicated the existence of a stable conformation of **3** more than 5 kcal/mol higher in energy than the lowest energy conformation. This conformation is too high in energy to contribute to the observable properties of **3** at room temperature and is consequently ignored here. The dihedral angles C1C2O8C9 of the B3LYP/TZ2P and B3PW91/TZ2P structures of **3a** are close to the angle C1C2O8H9 of conformation **b** of **1**, the O8−C9 bond lying between the C2−C3 and C2−H10 bonds.

In the cases of **4** and **5**, whatever the basis set and functional, only one stable conformation is predicted. The dihedral angles C1C2O8C9 and C1C2O8Si9 of the B3LYP/TZ2P and B3PW91/TZ2P structures of **4a** and **5a** are closest to the angle C1C2O8H9 of conformation **b** of **1**, the O8−C9 and O8−Si9 bonds lying between the C2−C3 and C2−H10 bonds.

Vibrational Spectra. We have measured the IR and VCD spectra of CCl_4 solutions of **1**, **3**, **4**, and **5** in the mid-IR spectral region, with the results shown in Figure 3. To analyze these spectra, we have calculated the IR and VCD spectra of **1**, **3**, **4**, and **5** at the B3LYP/TZ2P and B3PW91/TZ2P levels. In the cases of **3**, **4**, and **5**, the spectra are calculated for the single conformations **3a**, **4a**, and **5a**, respectively. In the case of **1**, spectra are calculated for all three conformations, **a**−**c**, and the conformationally averaged spectra obtained thence using the calculated relative free energies.

The B3LYP/TZ2P and B3PW91/TZ2P harmonic vibrational frequencies, dipole strengths, and rotational strengths of **5a** are given in Table 1 of the Supporting Information. The IR and VCD spectra derived thence using Lorentzian band shapes are shown in Figure 1 of the Supporting Information, together with the experimental spectra of **5**, and demonstrate that the B3PW91 calculations yield superior overall agreement with experiment. Our analysis is therefore based on the B3PW91/TZ2P calculations. The B3PW91/TZ2P IR spectrum is in superb agreement with the experimental IR spectrum, leading straightforwardly and unambiguously to the assignment of the latter, as detailed in Figure 4 and in Table 2 of the Supporting Information. As usual, experimental frequencies are uniformly a few percent lower than calculated frequencies due to the absence of anharmonicity in the calculations.[1a,b,2a−h,7] Absolute and relative intensities of the experimental IR spectrum are well reproduced by the calculated spectrum. Equally good agreement between the B3PW91/TZ2P and the experimental VCD spectra is observed. The assignment of the VCD spectrum of **5** is detailed in Figure 5 and in Table 2 of the Supporting Information. The excellent agreement

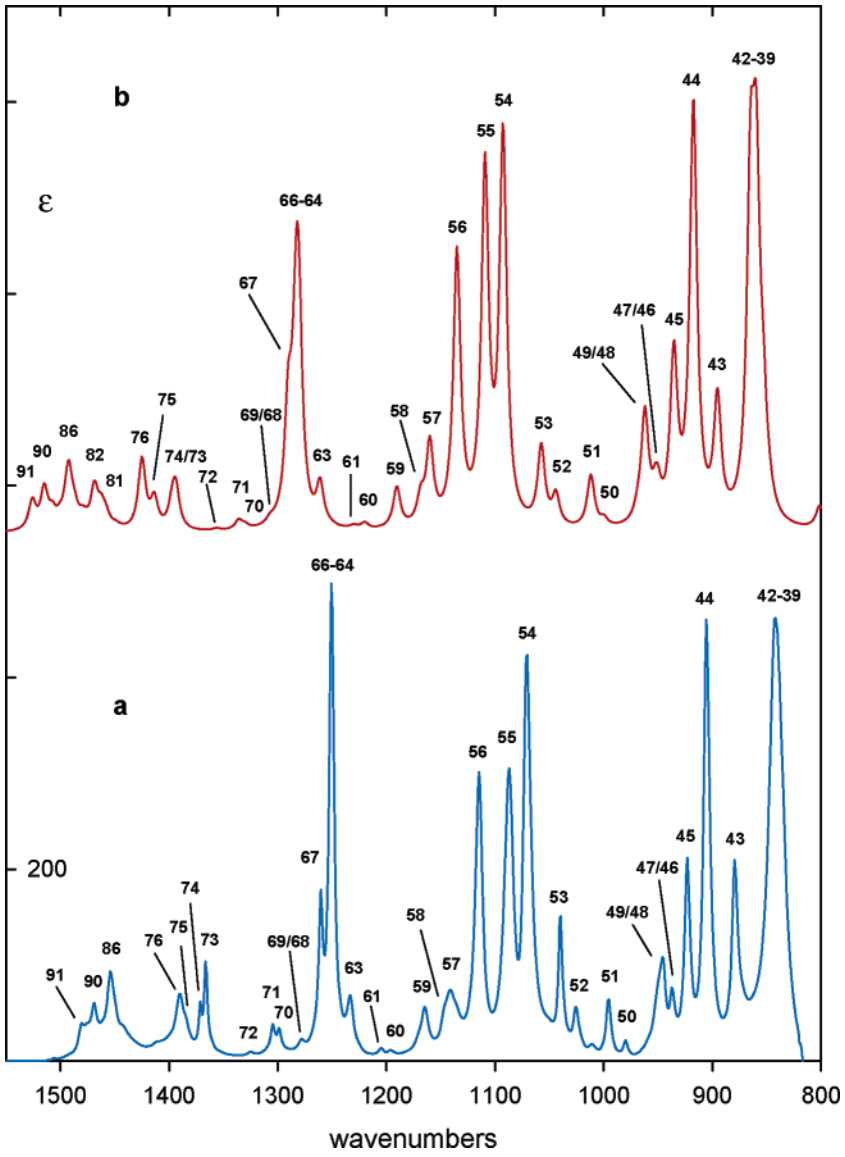

FIGURE 4. Comparison of the B3PW91/TZ2P IR spectrum of **5a** (spectrum **b**, red) to the experimental IR spectrum of (+)-**5** (spectrum **a**, blue) (from Figure 3). Fundamentals are numbered.

TABLE 2. Calculated and Experimental Specific Rotations $[\alpha]_D$ of 1, 3, 4, and 5

	calculated[a]			
	B3LYP/aug-cc-pVDZ// B3LYP/6-31G*	B3LYP/aug-cc-pVDZ// B3PW91/TZ2P	B3PW91/aug-cc-pVDZ// B3PW91/TZ2P	experiment[e]
1a	−5.8	−1.9	−1.4	+38.1 [*c* 4.67, 0.30 M], +37.8 [*c* 2.98, 0.19 M], +40.4 [*c* 0.47, 0.03 M], +41.5 [*c* 0.12, 0.008 M]
1b	+77.2	+72.8	+67.7	
1c	+76.4	+76.5	+73.9	
1[b]	+35.3[c]	+41.5[d]	+39.5[d]	
3a	+83.8	+74.4	+73.5	+40.8 [*c* 4.0, 0.20 M], +39.4 [*c* 3.53, 0.18 M], +42.2 [*c* 0.35, 0.018 M], +43.1 [*c* 0.09, 0.005 M].
4a	+58.5	+54.8	+53.1	+51.6 [*c* 3.23, 0.15 M], +54.8 [*c* 0.32, 0.015 M], +54.8 [*c* 0.08, 0.004 M].
5a	+60.6	+47.4	+45.1	+39.6 [*c* 3.4, 0.15 M], +41.1 [*c* 3.3, 0.14 M], +42.4 [*c* 0.34, 0.015 M], +39.5 [*c* 0.08, 0.004 M].

[a] 1*R*,2*S*,4*R* AC. [b] Conformationally averaged specific rotations. [c] Average based on B3LYP/6-31G* ΔG values. [d] Average based on B3PW91/TZ2P ΔG values. [e] In CCl_4 solution.

of calculated and experimental IR and VCD spectra for **5** demonstrates unambiguously that only one conformation of **5** contributes to the experimental spectrum and that the structure of that conformation is very well described by the B3PW91/TZ2P structure of conformation **5a**. In addition, one may note that the agreement of calculated and experimental VCD confirms the 1*R*,2*S*,4*R*-(+) absolute configuration of **5**.

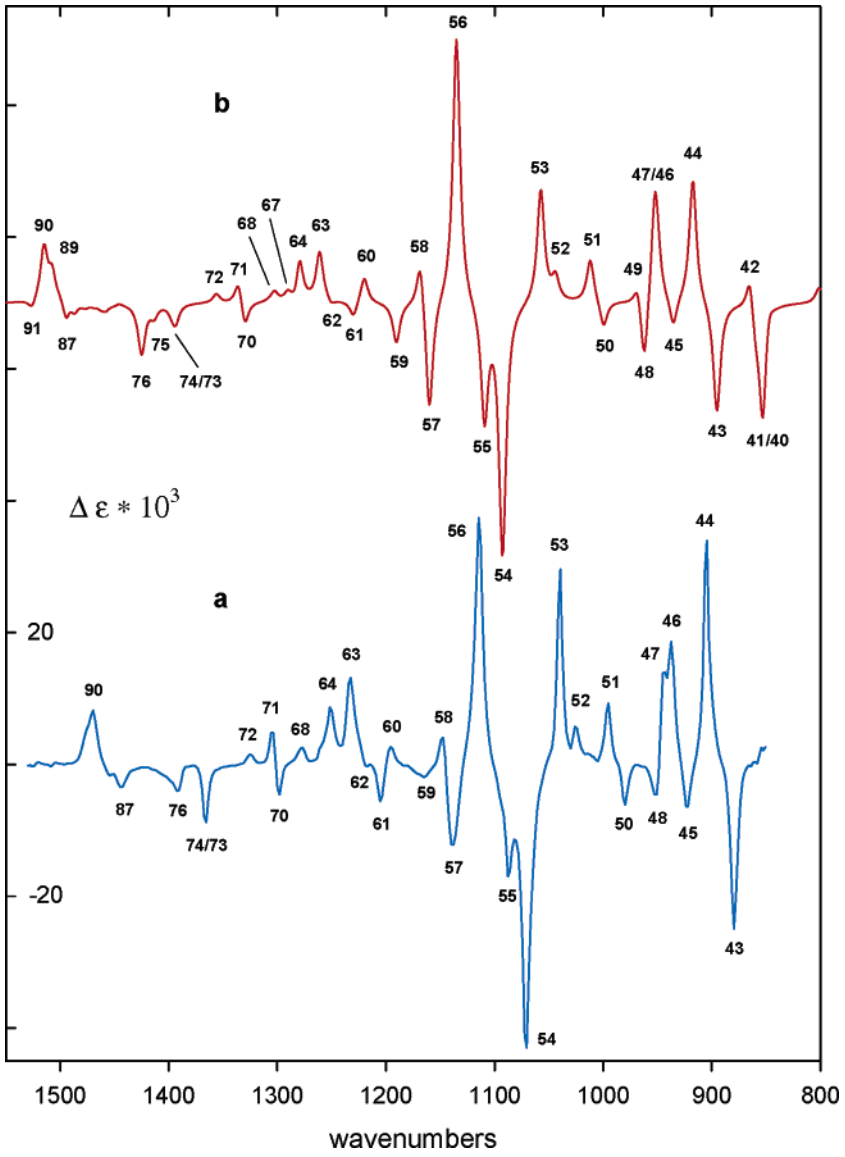

FIGURE 5. Comparison of the B3PW91/TZ2P VCD spectrum of (1*R*,2*S*,4*R*)-**5a** (spectrum **b**, red) to the experimental VCD spectrum of (+)-**5** (spectrum **a**, blue) (from Figure 3). Fundamentals are numbered.

The B3LYP/TZ2P and B3PW91/TZ2P harmonic vibrational frequencies, dipole strengths, and rotational strengths of **4a** are given in Table 3 of the Supporting Information. Comparison of the B3LYP/TZ2P and B3PW91/TZ2P IR and VCD spectra of **4a**, derived thence, to the experimental spectra of **4**, shown in Figure 2 of the Supporting Information, again demonstrates that the B3PW91 calculations are in clearly superior overall agreement with experiment. The B3PW91/TZ2P IR spectrum is in excellent agreement with the experimental IR spectrum, leading to the assignment of the latter, as detailed in Figure 6 and in Table 4 of the Supporting Information. The B3PW91/TZ2P and the experimental VCD spectra are also in excellent agreement; the assignment is detailed in Figure 7 and Table 4 of the Supporting Information. As with **5**, the excellent agreement of calculated and experimental IR and VCD spectra for **4** demonstrates unambiguously that only one conformation of **4** contributes to the experimental spectrum and that the structure of that conformation is well-described by the B3PW91/TZ2P structure of **4a**.

The B3LYP/TZ2P and B3PW91/TZ2P harmonic vibrational frequencies, dipole strengths, and rotational strengths of **3a** are given in Table 5 of the Supporting Information. Comparison of the B3LYP/TZ2P and B3PW91/TZ2P IR and VCD spectra of **3a**, derived thence, to the experimental spectra of **3** is shown in Figure 3 of the Supporting Information. While the agreement of calculated and experimental spectra is less different for the B3LYP and B3PW91 spectra than was the case for **5a** and **4a**, for consistency we analyze the spectra of **3** using the B3PW91/TZ2P calculations. The B3PW91/TZ2P IR and VCD spectra of **3a** are compared to the experimental spectra in Figures 8 and 9. Overall, the agreement is excellent and the assignment of the experimental spectra is straightforward, with the results detailed in Figures 8 and 9 and in Table 6 of the Supporting Information. Some differences exist in relative intensi-

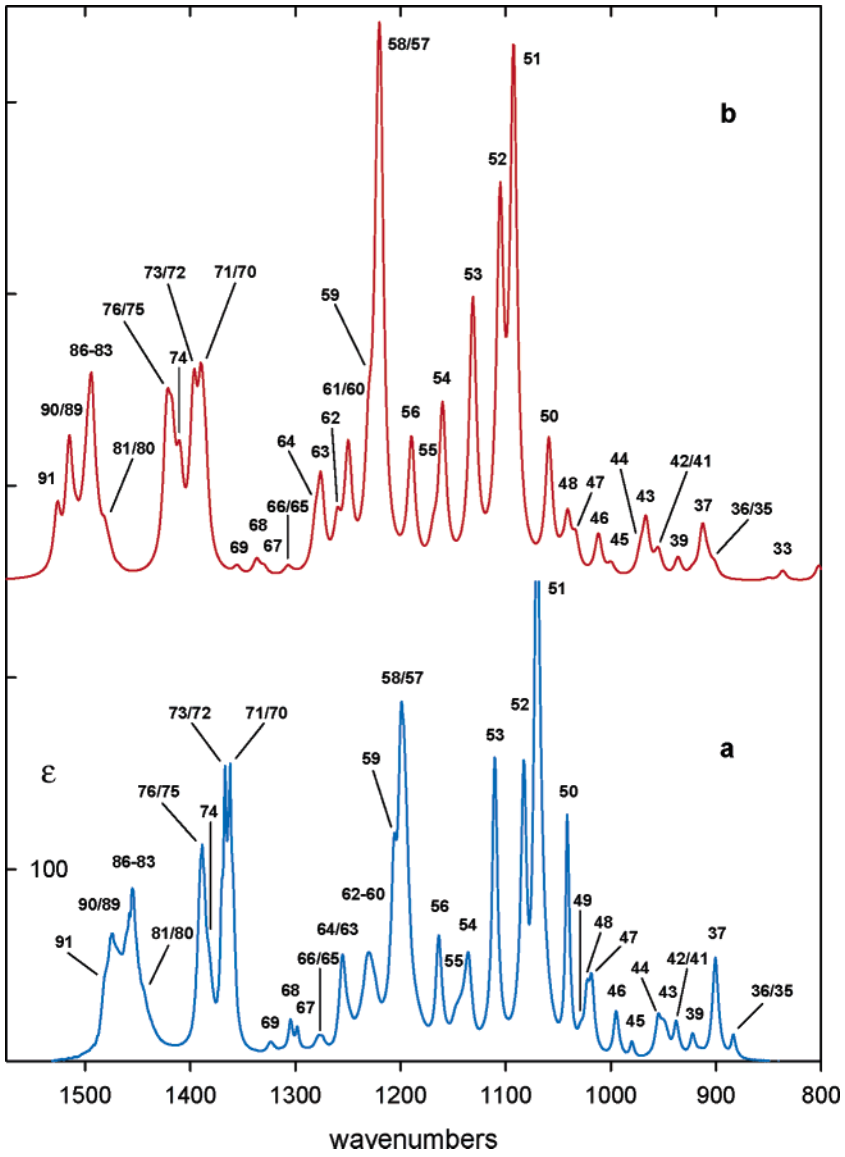

FIGURE 6. Comparison of the B3PW91/TZ2P IR spectrum of **4a** (spectrum **b**, red) to the experimental IR spectrum of (+)-**4** (spectrum **a**, blue) (from Figure 3). Fundamentals are numbered.

ties. For example, fundamentals 43 and 41/40 differ substantially in relative intensity in the IR spectrum (Figure 8). Similarly, the calculated VCD spectrum between fundamentals 49 and 55 differs substantially from that observed (Figure 9). Despite these limited differences, the overall agreement of calculated and experimental spectra supports the conclusion that only one conformation of **3** contributes to the experimental spectra and that its geometry is close to the B3PW91/TZ2P structure of conformation **3a**.

The analysis of the IR and VCD spectra of **1** is considerably more complicated due to the substantial population of all three conformers **a**−**c**. The B3PW91/TZ2P harmonic frequencies, dipole strengths, and rotational strengths of **1a**, **1b**, and **1c** are given in Table 7 of the Supporting Information. In Figure 10, the B3PW91/TZ2P IR and VCD spectra of conformations **1a**, **1b**, and **1c**, obtained thence, are superposed. In Figures 11 and 12, the conformationally averaged IR and VCD spectra obtained thence using populations calculated from B3PW91/TZ2P relative free energies (Table 1) are compared to the experimental spectra. The IR spectra and, especially, the VCD spectra of the three conformations of **1** vary substantially. As a result, the conformationally averaged spectra differ substantially from the spectra of any one individual conformation. Due to the substantial overlap of the spectra of the individual conformations, relatively few bands in the conformationally averaged spectra can be attributed to a single conformation. However, as detailed in Figures 11 and 12, bands 24c, 32a, 37b, 40b, 50a, 50b, and 54c are resolved in the IR spectrum, and bands 24a, 24c, 25c, 30c, 31b, 32a, 32c, 33b, 37c, 40b, 45c, 47b, 50c, 50a, 53b, 54b, and 54c are resolved in the VCD spectrum. The predicted IR and VCD spectra of **1** exhibit moderately good agreement with experiment, leading to the partial assignments detailed in Figures 11 and 12 and in Table 8 of the Supporting Information. Bands originating in fundamentals 24c, 32a, 37b, 40b, 50a, 50b, and 54c are identifiable in the experimental IR spectrum, providing evidence for the

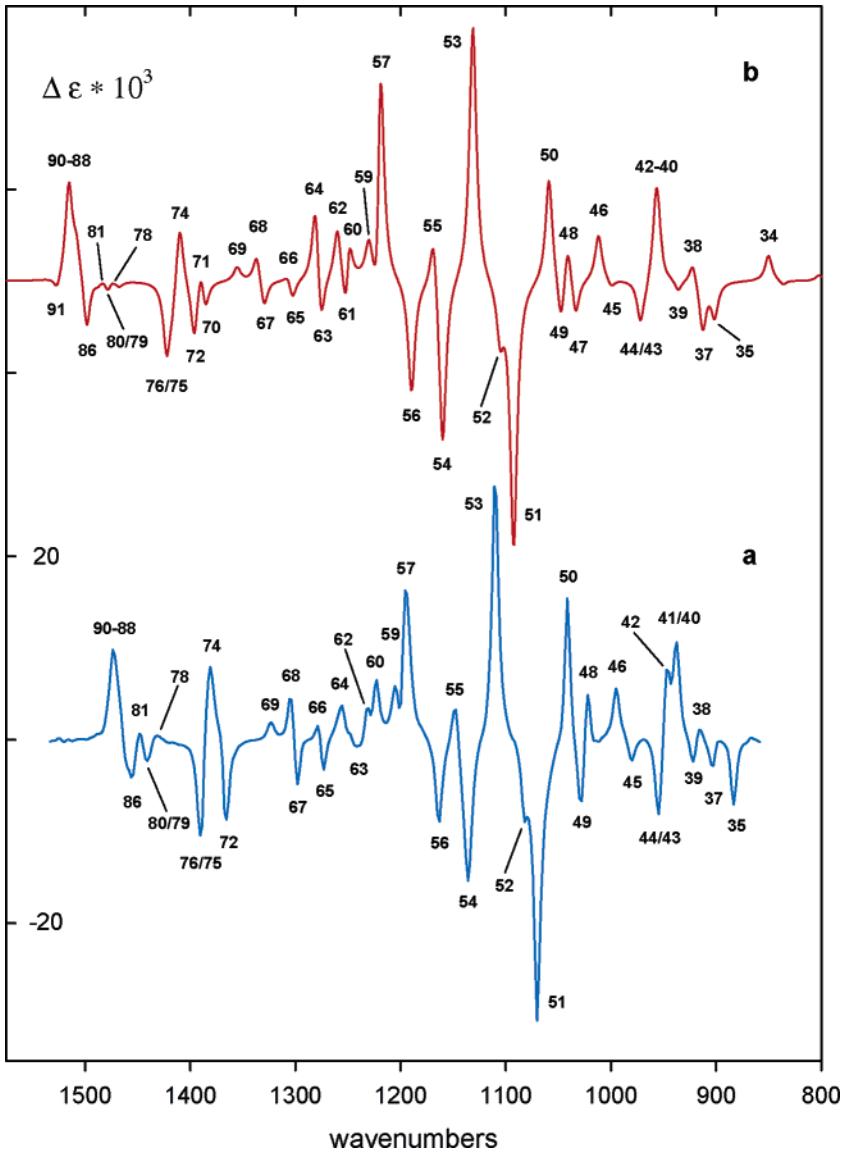

FIGURE 7. Comparison of the B3PW91/TZ2P VCD spectrum of (1*R*,2*S*,4*R*)-**4a** (spectrum **b**, red) to the experimental VCD spectrum of (+)-**4** (spectrum **a**, blue) (from Figure 3). Fundamentals are numbered.

contributions of all three conformations **1a**, **1b**, and **1c**. Likewise, bands originating in fundamentals 24c, 25c, 30c, 31b, 32a, 37c, 50c, 53b, and 54b are identifiable in the experimental VCD spectrum, adding further evidence for conformations **a**−**c**. Overall, the comparison of the calculated and experimental IR and VCD spectra of **1** support qualitatively the theoretical conformational analysis of **1**. However, quantitative deconvolution of the IR and VCD spectra would be required to obtain the experimental frequencies, dipole strengths, and rotational strengths for the three conformations and, thence, their relative free energies.[8] This has yet to be carried out.

The B3LYP/TZ2P harmonic vibrational frequencies, dipole strengths, and rotational strengths of **1a**−**c** are also given in Table 7 of the Supporting Information. Conformationally averaged B3LYP/TZ2P IR and VCD spectra derived thence are compared to the B3PW91/TZ2P spectra and to the experimental spectra of **1** in Figure 4 of the Supporting Information. Overall, the spectra obtained from the two functionals are similar. Differences exist in detail, but neither functional gives clearly superior agreement with experiment.

The experimental IR and VCD spectra of **1**, **3**, **4**, and **5** discussed above have been measured at concentrations in the range 0.1−0.2 M. In order to define the extent to which intermolecular interactions cause aggregation at these concentrations, we have measured the IR spectra at several concentrations in the range 0.001−1 M, with the results shown in Figures 5−9 of the Supporting Information. In the cases of **3**, **4**, and **5**, Beer's Law is obeyed within experimental error, demonstrating that aggregation is negligible. In the case of **1**, significant concentration dependence is observed, especially in the

(8) (a) Devlin, F. J.; Stephens, P. J. *J. Am. Chem. Soc.* **1999**, *121*, 7413−7414. (b) Aamouche, A.; Devlin, F. J.; Stephens, P. J. *J. Am. Chem. Soc.* **2000**, *122*, 7358−7367. (c) Devlin, F. J.; Stephens, P. J.; Scafato, P.; Superchi, S.; Rosini, C. *J. Phys. Chem. A* **2002**, *106*, 10510−10524.

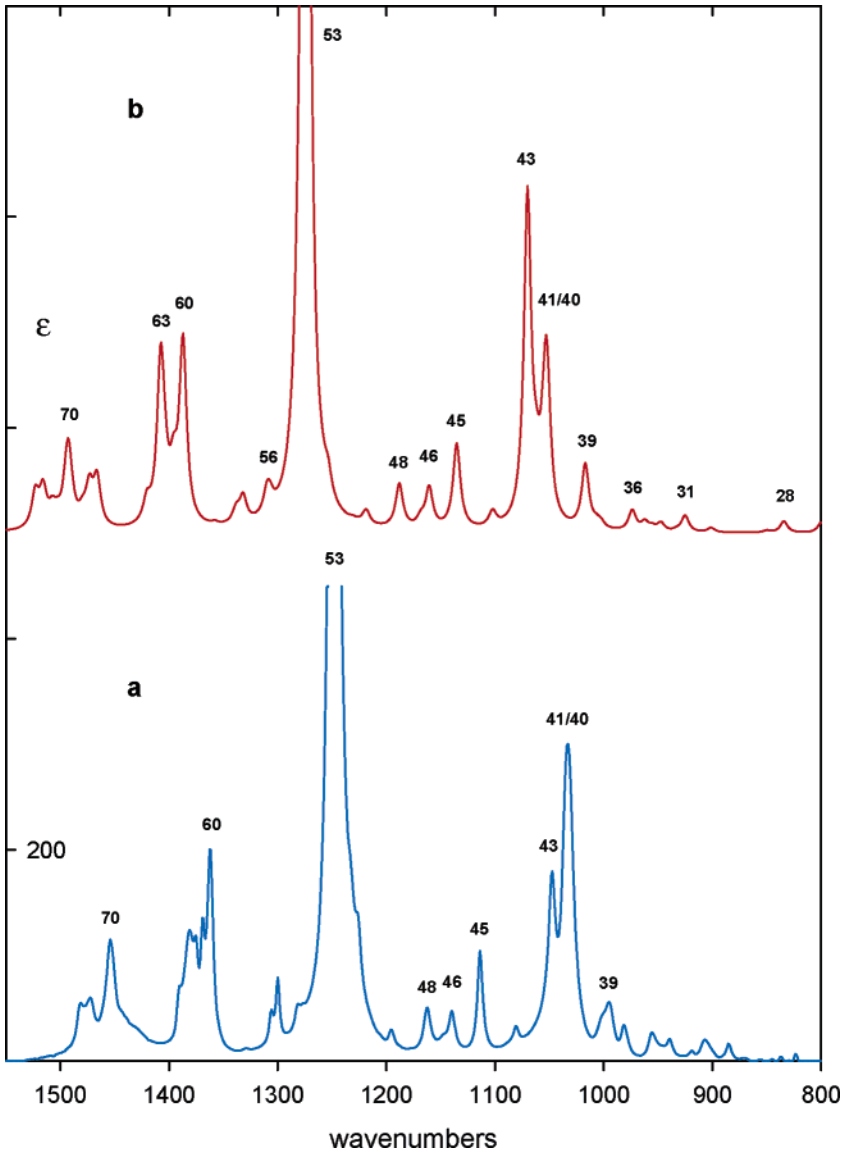

FIGURE 8. Comparison of the B3PW91/TZ2P IR spectrum of **3a** (spectrum **b**, red) to the experimental IR spectrum of (+)-**3** (spectrum **a**, blue) (from Figure 3). Fundamentals are numbered.

O−H stretching region, demonstrating the occurrence of aggregation. Taking the broad O−H stretching absorption at 3200−3600 cm^{-1} as a gauge, aggregation is significant at concentrations >∼0.01 M. In the mid-IR spectral region, modest concentration dependence is observed. Apparently, the IR spectrum in this region is not extremely sensitive to aggregation. This is consistent with the moderately good agreement of the IR and VCD spectra calculated for the isolated borneol molecule with the experimental spectra at ∼0.2 M.

Optical Rotation. We have examined the concentration dependence of the experimental $[\alpha]_D$ values of **1**, **3**, **4**, and **5** with the results given in Table 2. As expected from the concentration dependence of their IR spectra, for **3**, **4**, and **5** the concentration dependence of $[\alpha]_D$ is minor and the variation is probably within experimental error (especially at the lowest concentrations). Unexpectedly, the concentration dependence of $[\alpha]_D$ for **1** is also small, indicating that the aggregation demonstrated by IR spectroscopy to occur with increasing concentration does not markedly affect $[\alpha]_D$, a surprising result.

We have calculated the specific rotations $[\alpha]_D$ of **1**, **3**, **4**, and **5** using the B3LYP and B3PW91 functionals, the aug-cc-pVDZ basis set, and the B3LYP/6-31G* and B3PW91/TZ2P equilibrium geometries, with the results given in Table 2. In the case of **1**, conformationally averaged $[\alpha]_D$ values are obtained using relative free energies. The $[\alpha]_D$ values of **4** and **5** calculated at the B3PW91/TZ2P geometries are in excellent agreement with the observed $[\alpha]_D$ values: the differences are <10. Only slightly worse agreement is obtained when $[\alpha]_D$ is calculated at the B3LYP/6-31G* geometries. For **3**, the quantitative agreement is less good: the differences between calculated and experimental $[\alpha]_D$ values are >30 and >40 at the B3PW91/TZ2P and B3LYP/6-31G* geometries, respectively. In the case of **1**, the conformationally averaged $[\alpha]_D$ is in exceptionally good agreement

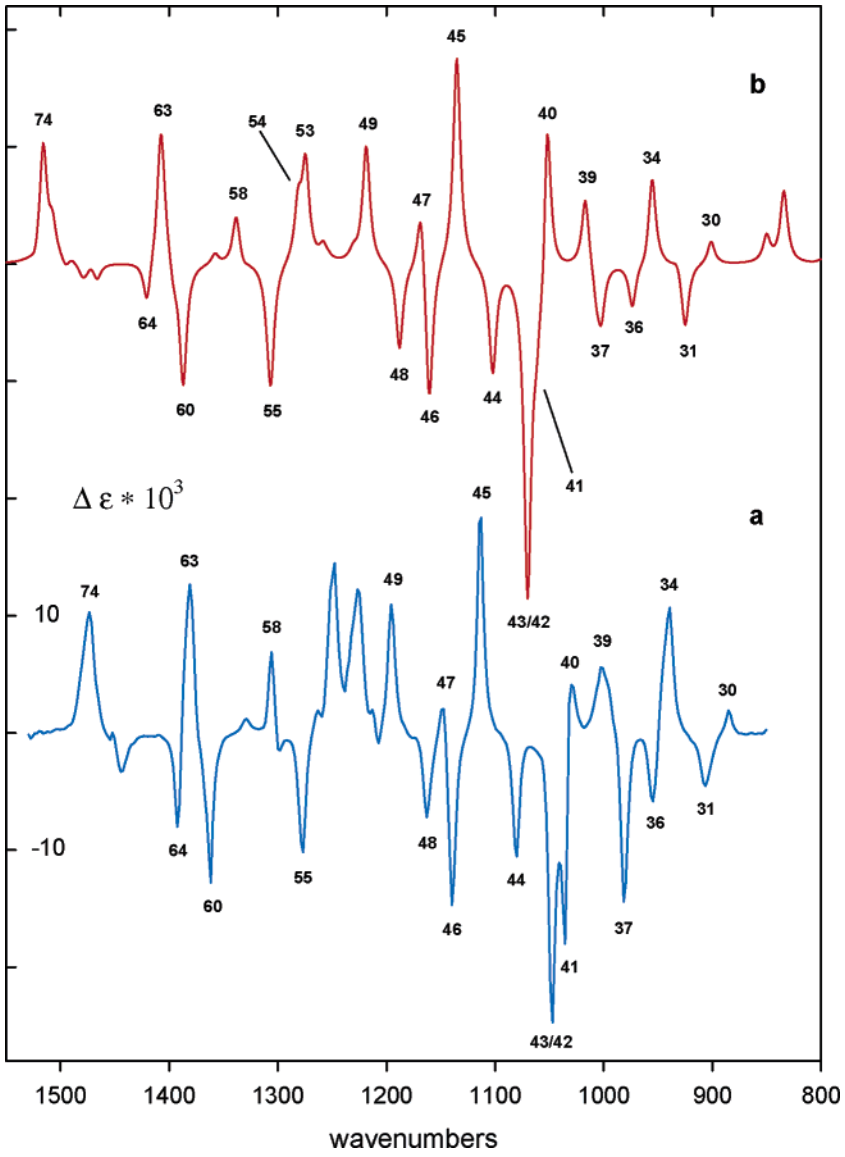

FIGURE 9. Comparison of the B3PW91/TZ2P VCD spectrum of (1*R*,2*S*,4*R*)-**3a** (spectrum **b**, red) to the experimental VCD spectrum of (+)-**3** (spectrum **a**, blue) (from Figure 3). Fundamentals are numbered.

with experiment. This is extremely surprising since $[\alpha]_D$ varies considerably in magnitude from **1a**−**1c** and also changes sign. The excellent agreement is therefore undoubtedly fortuitous.

Discussion

As anticipated, B3LYP/6-31G* DFT calculations predict the existence of three stable conformations of *endo*-borneol, **1a**, **1b**, and **1c**, corresponding to the three staggered conformations of the O−H group. The energies of **1a**, **1b**, and **1c** are very similar, spanning a range of <1 kcal/mol. The barriers to internal rotation of the O−H group are also small: from the minimum to the maximum on the PES is <3 kcal/mol. At room temperature, *endo*-borneol therefore is predicted to exist as an equilibrium mixture of all three conformations. The experimental IR and VCD spectra of borneol are consistent with this expectation. The conformationally averaged B3PW91/TZ2P spectra are in good agreement with the experimental spectra. A number of observed bands can be assigned to fundamentals of a single conformation, demonstrating conclusively that all three conformations do indeed contribute to the spectra.

Our principal goal here is to examine the extent to which derivatization of the OH group of borneol reduces its conformational flexibility and, specifically, the number of stable conformations. Computationally, we have examined four derivatives in which the OH H atom is replaced by CH_3, $COCH_3$, $C(CH_3)_3$, and $Si(CH_3)_3$ groups, respectively. Even with the smallest substituent, CH_3, derivatization markedly changes the B3LYP/6-31G* PES, showing that the steric hindrance to rotation of the CH_3 group is far greater than for the H atom. The number of stable conformations is reduced to two; their energy difference is substantially greater than the differences between the conformations of **1**. The B3LYP/6-31G* PES for the acetate derivative, **3**, is quite similar overall to that of **2**. However, in detail there are differences reflecting the differences between CH_3 and $COCH_3$ groups. A double minimum PES is observed, with a very

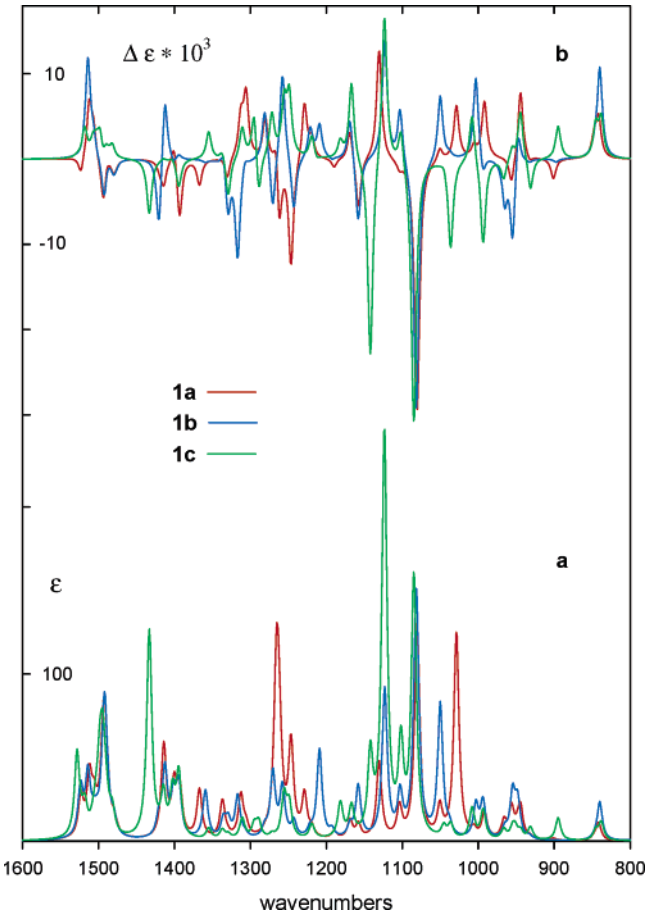

FIGURE 10. B3PW91/TZ2P IR (a) and VCD (b) spectra of **1a**, **1b**, and **1c**.

small barrier between two stable conformations. At the TZ2P basis set level, for both functionals B3LYP and B3PW91, the barrier is reduced to such an extent that only one of these conformations survives as a stable conformation. We also predict a further stable conformation at much higher energy (>5 kcal/mol), but this is not of consequence for the observable room-temperature properties of **3**. The $C(CH_3)_3$ and $Si(CH_3)_3$ groups are substantially more bulky than the CH_3 and $COCH_3$ groups and lead to PESs with a single minimum, i.e., the number of stable conformations is reduced to one. The steepness of the valley in the PES is greater for **4** than for **5**, as is the barrier to internal rotation, indicating greater steric hindrance to rotation of the $C(CH)_3$ group than for the $Si(CH_3)_3$ group. This difference is attributable to the greater length of the O−Si bond of **5** (1.678 Å) compared to the O−C bond of **4** (1.444 Å), which therefore places its methyl groups at a greater distance from the rest of the molecule.

The experimental IR and VCD spectra of **3**−**5** confirm our predictions that all three molecules exhibit a single stable conformation. Comparison of the B3PW91/TZ2P IR and VCD spectra of **4** and **5** to the corresponding experimental spectra permits unambiguous assignment of the experimental spectra. There is no evidence of additional bands which would support the identification of a second conformation. The same conclusion applies to **3**, although the agreement of predicted and experimental spectra is not quite as excellent as in the cases of **4** and **5**. Thus, complete vibrational analysis of the IR and VCD spectra of **3**, **4**, and **5** is enormously simpler than for **1** due to the reduction in the number of populated conformations from three to one on derivatization of the O−H group of **1**.

It is clear that significant rigidification of alcohols can be achieved by derivatization of their OH groups. [We recognize, of course, that the degree of rigidification achieved by derivatization will depend on the specific molecule concerned.] Our results lead to the conclusion that, of the derivatives considered here, maximum rigidification is achieved in *tert*-butyl derivatives and this is likely to be the most useful derivative. However, both the trimethylsilyl and acetate derivatives achieve a similar level of rigidification and appear to be useful. On the other hand, our computational results indicate that the methyl derivatives are significantly less rigid and, therefore, less useful. From a practical point of view, preparation of acetate and trimethylsilyl derivatives is normally routine, while *tert*-butyl derivatives are somewhat less routinely synthesized. In this work, we have used the procedure of Armstrong et al.[4] involving reaction with *tert*-butyl trichloroacetamidate. When this procedure is not effective, alternatives such as reaction with isobutylene[9] exist.

We have demonstrated the rigidification of *endo*-borneol on derivatization via the IR and VCD spectroscopic techniques. Vibrational spectroscopy is exquisitely sensitive to molecular structure, and the concerted use of IR and VCD in combination with DFT calculations provides a powerful methodology for conformational analysis of chiral molecules.[2a,8] The excellent agreement of predicted and experimental IR and VCD spectra of **3**−**5** unambiguously proves their rigidity and confirms the structures of these derivatives predicted by DFT.

In view of the recent development of the TDDFT/GIAO technique for calculating transparent spectral region specific rotations of chiral molecules,[1c,d] we have also measured and calculated the sodium D line specific rotations of **1**, **3**, **4**, and **5**. We anticipated that calculated $[\alpha]_D$ values would be in best agreement with experimental values for the conformationally rigid derivatives **3**, **4**, and **5** and in less good agreement for **1**. We indeed found good agreement for **3**, **4**, and **5**, but in the case of **1** agreement was also excellent, a surprising and probably fortuitous result.

A fringe benefit of derivatizing the OH group of an alcohol is the elimination of intermolecular H-bonding at medium-to-high concentrations in nonpolar solvents. Via measurement of the concentration dependence of the IR spectra of **1**, **3**, **4**, and **5**, we have documented the existence of increasing aggregation with increasing concentration over the millimolar-to-molar concentration range in the case of **1** and its absence in the cases of **3**, **4**, and **5**. Accordingly, the analyses of the IR and VCD spectra of **3**, **4**, and **5** measured at >0.1 M concentrations can be carried out on the basis of calculations for isolated molecules. In the case of **1**, the demonstrated existence of significant aggregation at the >0.1 M concentration of the IR and VCD experiments leads to the expectation

(9) Alexakis, A.; Gardette, M.; Colin, S. *Tetrahedron Lett.* **1988**, *29*, 2951−2954.

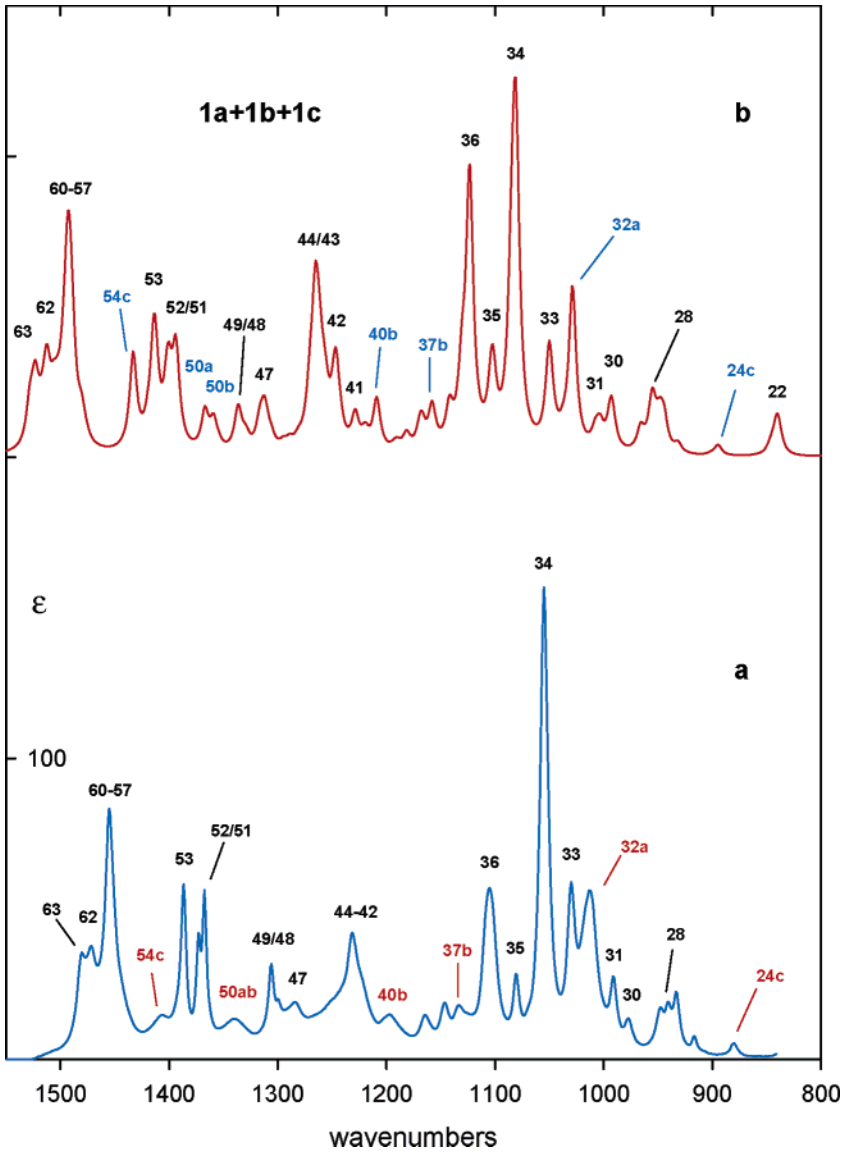

FIGURE 11. Comparison of the conformationally averaged B3PW91/TZ2P IR spectrum of **1** (spectrum **b**, red) to the experimental IR spectrum of (+)-**1** (spectrum **a**, blue) (from Figure 3). Equilibrium populations were obtained from B3PW91/TZ2P relative free energies (Table 1). Fundamentals are numbered. Bands attributable to a single conformation of **1** are highlighted.

that calculations for isolated molecules of **1** will exhibit reduced agreement with experimental spectra. Agreement is indeed less good for **1** than for **3**, **4**, and **5**. Whether this is predominantly due to the greater conformational flexibility of **1** or the contributions of aggregate forms of **1** remains to be established.

The use of chemical derivatization in studies of ACs of chiral molecules via chiroptical spectroscopic techniques is not new. Derivatization has been widely used in applications of the exciton coupling (coupled oscillator) methodology to determine ACs via electronic CD spectroscopy.[10] The purpose there, however, is to create CD signals capable of analysis, and not conformational rigidification. Derivatization has also been used in applications of VCD spectroscopy to AC determination in the case of chiral molecules with COOH groups. The formation of the methyl esters of such molecules inhibits aggregation via intermolecular H-bonding of COOH groups and enables experimental data to be analyzed on the basis of isolated molecule calculations, rather than calculations for dimer molecules. Recent examples of this approach include our studies of the ACs of spiropentyl carboxylic acid[2g] and of several phenyl glycidic acids.[11]

Conformational rigidification via chemical derivatization was used in studies of the ACs of diols via electronic CD spectroscopy.[12] However, to date, this methodology has not been systematically employed in determining ACs via chiroptical spectroscopy. We hope that the present study will stimulate a wider range of applica-

(10) Harada, N.; Nakanishi, K. *Circular Dichroic Spectroscopy: Exciton Coupling in Organic Stereochemistry*; University Science Books: 1983.

(11) Devlin, F. J.; Stephens, P. J.; Bortolini, O. In preparation.

(12) (a) Rosini, C.; Scamuzzi, S.; Uccello-Barretta, G.; Salvadori, P. *J. Org. Chem.* **1994**, *59*, 7395−7400. (b) Pini, D.; Mandoli, A.; Iuliano, A.; Salvadori, P. *Tetrahedron: Asymmetry* **1995**, *6*, 1031−1034.

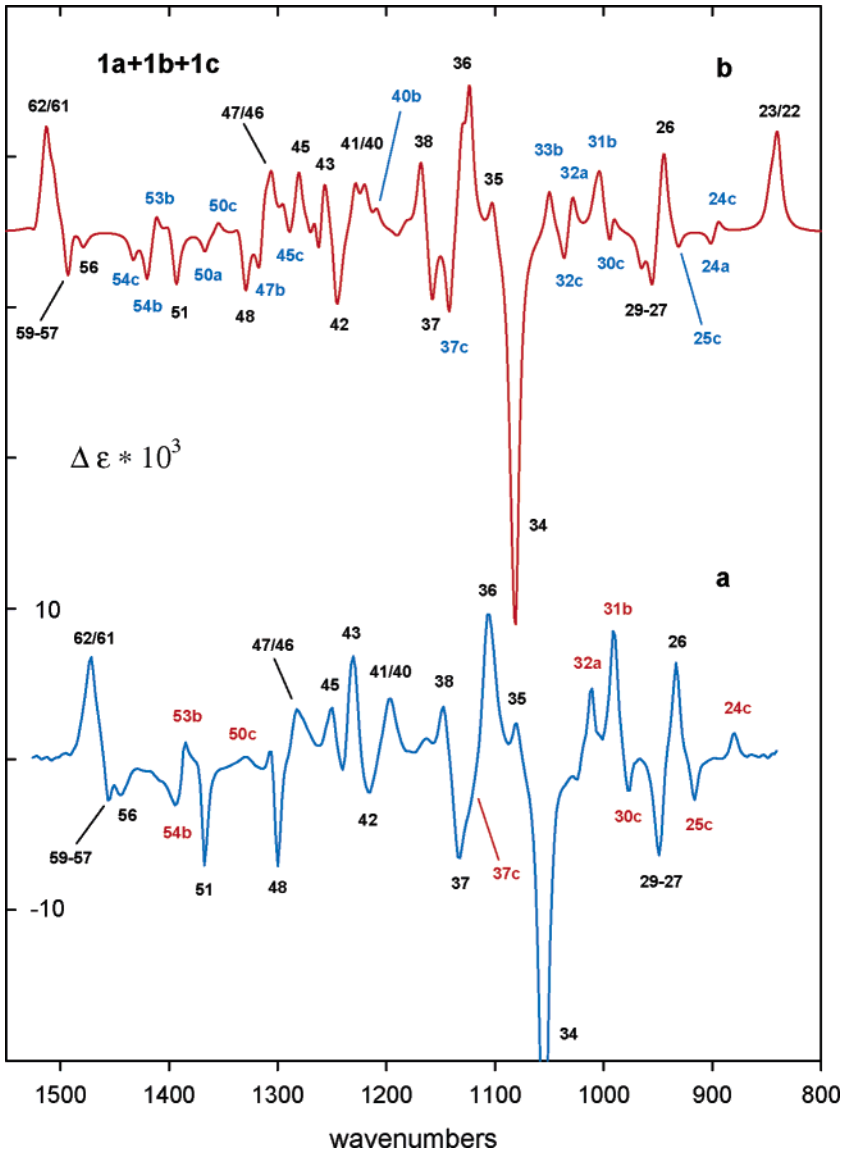

FIGURE 12. Comparison of the conformationally averaged B3PW91/TZ2P VCD spectrum of (1*R*,2*S*,4*R*)-**1** (spectrum **b**, red) to the experimental VCD spectrum of (+)-**1** (spectrum **a**, blue) (from Figure 3). Equilibrium populations were obtained from B3PW91/TZ2P relative free energies (Table 1). Fundamentals are numbered. Bands attributable to a single conformation of **1** are highlighted.

tions, making use of a wide range of functional groups (and functional group combinations) and of derivatives thereof.

As a result of our study of derivatives of *endo*-borneol, we have exploited the conformational rigidification through chemical derivatization methodology in determining the ACs of 2-(1-hydroxyethyl)-chromen-4-one and its 6-Br derivative.[13] Studies of the VCD spectra of their acetate and *tert*-butyl derivatives have unambiguously defined their ACs.[14]

Acknowledgments. We acknowledge financial support of this research by the National Science Foundation (Grant CHE-0209957 to P.J.S.). We are also grateful to the USC Center for High Performance Computing for computer time and to H. Veschambre for assistance.

Supporting Information Available: Harmonic frequencies, dipole strengths, and rotational strengths; comparison of B3PW91/TZ2P, B3LYP/TZ2P, and experimental IR and VCD spectra; assignments of experimental IR and VCD spectra; concentration dependence of the IR spectra; Cartesian coordinates of optimized geometries; and synthesis and characterization. This material is available free of charge via the Internet at http://pubs.acs.org.

JO0478611

(13) Besse, P.; Baziard-Mouysset, G.; Boubekeur, K.; Palvadeau, P.; Veschambre, H.; Payard, M.; Mousset, G. *Tetrahedron: Asymmetry* **1999**, *10*, 4745−4754.

(14) Devlin, F. J.; Stephens, P. J.; Besse, P. *Tetrahedron: Asymmetry*, in press.